Hydrided Zircaloy-4 cladding failure criteria during Reactivity-Initiated Accidents

Katheren R.B. Nantes,* Miaomiao Jin,* and Arthur T. Motta,*

*Ken and Mary Alice Lindquist Department of Nuclear Engineering, The Pennsylvania State University, University Park, PA, krn5198@psu.edu, mmjin@psu.edu, atm2@psu.edu

doi.org/10.13182/T130-44826

INTRODUCTION

The a common material used for fuel cladding of nuclear reactors is Zircaloy-4, due to its favorable properties as corrosion resistance, low neutron absorption cross-section and mechanical properties under normal operating conditions [1]. In Light Water Reactors (LWR), Zircaloy can still be corroded by the contact with water coolant, which leads to absorption of hydrogen into the metal lattice.

This absorbed hydrogen can undergo redistribution driven by concentration gradient (Fick's law of diffusion), temperature gradient (Soret effect or thermophoresis), and hydrostatic stress gradient. The overall hydrogen flux is mathematically represented in Equation 1, where D_H denotes the diffusion coefficient of hydrogen in Zr, C_{ss} is the concentration of hydrogen in solid solution in α-Zr, Q^* is the heat of transport of hydrogen in Zr, T is the temperature, R is the ideal gas constant, V is the molar volume of hydrogen in Zr, and $\nabla\sigma_H$ is the hydrostatic stress gradient.

$$J_H = -D_H \nabla C_{ss} - D_H \frac{Q^* C_{ss} \nabla T}{RT^2} + D_H \frac{C_{ss} V}{RT} \nabla \sigma_H, \quad (1)$$

Breaking down Equation 1, the first term represents Fick's law of diffusion, meaning the flux goes against the concentration gradient, tending to homogenize the hydrogen in solution. The second term accounts for the Soret effect, and indicates that the hydrogen tends to go against the gradient. The third term represents the impact of hydrostatic stress gradient on hydrogen flux, leading to hydrogen accumulation in high-stress regions.

In a reactor environment, the Soret effect is more influential compared to the other two, causing hydrogen accumulation in colder regions and potential localization of zirconium hydride. This can adversely affect cladding ductility, potentially leading to early brittle failure due to internal stresses from operation, thermal stresses from accidents, or mechanical impact.

The Reactivity-Initiated Accident (RIA) is a design basis accident, characterized by a sudden reactivity increase in the core caused by the removal of a control rod [2]. During RIA, the fuel rods around the ejected control rod will have more neutrons available for fission reaction, therefore reactivity increases, leading to elevated fuel temperature, and expansion of the fuel pellets against the cladding. The combination of this stress condition and the hydride localization in the cladding can cause cracking of the hydrides at much lower stress than the Zircaloy, as they are more brittle.

As the industry have an interest in increase the burnup of fuel rods, the results from RIA experiments from various facilities around the world [2, 3, 4],indicate that high burnup fuel rods are prone to fail much earlier than expected by the current enthalpy criteria, and therefore, suggest a need for revision.

Numerical criteria to predict cladding failure during RIA were developed, among others, by Clifford [5] and Jernkvist [6], who derived their criteria by fitting curves to the RIA experimental distributions. However, those methods uses the cladding average hydrogen content and do not account for hydride localization, such as rim or blister formation and their depths, which has been shown in [7] to be very important when analysing cladding low-temperature failure. Therefore, this work intend tho present a new modeling failure criteria for hydrided Zircaloy that is being developed, and intend to account for hydride localization due to thermal gradients.

METHODS

The model here presented is based on the experimental work of Daum [8], who tested unirradiated hydrided Zircaloy-4 cladding under biaxial tension for both, uniformly distributed circumferential hydrides and hydride rim configurations. Then, we estimated two equations, one correlates the failure strain and the average hydride distribution, Equation 2, and another estimates failure strain as a function of hydride rim thickness, Equation 3.

$$\epsilon_f = 0.07425 - 3.1462 \times 10^{-5} C_H \quad (2)$$

$$\epsilon_f = 0.06332 - 2.5468 \times 10^{-4} t_{RIM}, \quad (3)$$

where ϵ_f is the estimated failure strain, the hydrogen concentration C_H is in wppm, and the rim thickness t_{RIM} is in μm and can be estimated by Equation 4 :

$$t_{RIM} = \frac{C_H(t)}{2700}[L_{clad} - t_{oxide}], \quad (4)$$

where $C_{ZrH}(t)$ is the radial average hydrogen concentration at time t at a certain cladding height, L_{clad} is the cladding initial thickness, and t_{oxide} is the oxide thickness at time t at the same height. The denominator 2700 is the hydride concentration expected at the rim, which was also estimated by Daum.

Assuming that the elastic strain was recovered at the time of measurement, the minimum strain to be measured is the one when the material starts yielding, so a lower limit for failure strain was estimated, using Equation 5, where, E is the elastic modulus for Zircaloy-4 at 300 ^{o}C, E = 78 GPa [9], and ϵ is the strain. The left side of this equation represents the elastic curve at the 0.2% offset used to estimate the yield stress, and the right side represents the plastic curve, which was estimated by Link [10]. Solving Equation 5, we estimate $\epsilon = 0.00763$. Then, we consider that $\epsilon_f = 0.00763$ for any ϵ_f estimated by Equation 2 or 3 that is lower than 0.00763. However, we should note that this limit was estimated using Zircaloy-4 parameters, an estimation using zirconium hydride parameters was also done and found to be $\epsilon_f = 0.005$, in reality, the limit should be in between these values.

$$E(\epsilon - 0.002) = 585\epsilon^{0.059}, \quad (5)$$

The model was implemented in the Nuclear Fuel Performance Code BISON [11], which is based on the MOOSE framework. The validation was conducted through simulations of the tests REP-Na3, REP-Na4, REP-Na5, and REP-Na10, which were conducted at the CABRI facility in Cadarache, France [2]. All the tests had the basic same modeling condition for a rodlet, using a 2D-axisymmetric mesh considering discrete fuel pellets, the main modeling parameters are shown in Table I. The differences of each test model are the height of fuel stacking, axial peaking factors, linear power history during normal operation and power pulse characteristics. The specific parameters of each test are shown in Table II. For all tests was performed first a rodlet pre-irradiation simulation in a normal PWR operation up to the desired burnup, then a second simulation is done for the power pulse using the pre-irradiation output with sodium coolant, as the CABRI REP-Na experiments were done using the test reactor sodium loop.

TABLE I. General BISON modeling parameters.

Fuel type	UO_2
Cladding type	Zircaloy-4
Coolant type	Sodium
Initial enrichment	4.5 (^{235}U/U%)
Initial Plenum Gas type	He
Initial Gas Pressure	2.6 MPa
Fuel Pellet diameter	8.19 mm
Fuel-cladding gap	82 μm
Fuel-cladding top gap	0.032 m
Fuel-cladding bottom gap	0.003 m
Top and bottom clad thickness	0.0015 m
Chamfer height	0.5 mm
Chamfer width	0.55 mm
Dish depth	0.205 mm
Dish radius	3 mm
Inlet Coolant Temperature	588.7 K
Fuel emissivity	0.798 [12]
Cladding emissivity	0.325 [13]

To consider the hydride blister formation after an oxide spallation, another equation was estimated to correlate the failure strain with the hydride blister depth. Equation 6 was estimated from the experiments performed by Glendening [14], equal biaxial tension tests of Zircaloy-4 sheets with different hydride blister depth at 300 ^{o}C. This correlation is to be validated through simulations of the CABRI REP-Na1 and REP-Na8 tests, as those presented localized oxide spallation and deep hydride blisters as main cause of cladding failure.

$$= 0.2136 - 0.0008 \times B_d \quad (6)$$

RESULTS AND ANALYSIS

On the validation of the proposed model, the comparison of simulated and CABRI experimental results, was use the deposited energy at the power peak node when failure happened, i.e. the integral under the power pulse curve from start until failure. From the validation simulations, on the non-failed experiments, REP-Na3, REP-Na4, and REP-Na5, our model did predict failure. For the REP-Na10 test, the model predicted failure at 69.6 cal/g of deposited energy at the power peak node, which has a 5.78% deviation from the value reported, shown in Table II. When performing the same simulation for REP-Na10, but using the Clifford model, which is the current one available in BISON, it presents failure at 80.2 cal/g of energy deposited at the power peak node, 21.9% of deviation from the experiment. Figure 1 shows the power pulse applied on the REP-Na10 test modeling, and the times when each model was triggered.

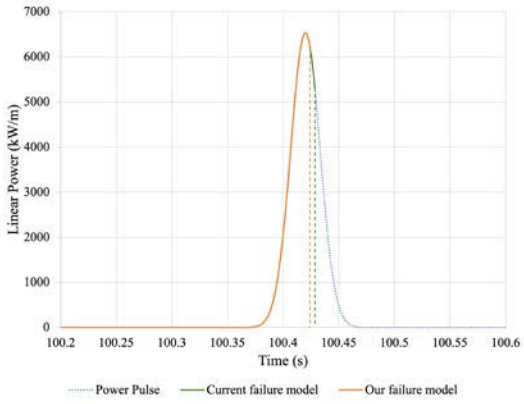

Fig. 1. Comparison between the failure prediction of current BISON RIA failure criteria and our model for the CABRI REP-Na10 test. The dashed lines represent the moment when the models predicted first failure.

CONCLUSIONS

Reactivity-Initiated Accidents are a postulated accident, in which the cladding can fail due to the stresses imposed by the Pellet-Cladding Mechanical Interaction. On high burnup fuel rods, it is very important to consider the hydride localizations that happen during cladding service, as the hydrides are more brittle than the Zircaloy metal and decrease the cladding overall ductility, inducing early failures. The model presented here, aims to predict cladding failure considering the hydride rim and hydride blisters formation in the cladding, differently from most model available in the literature. From the validation simulations we can say that our model is already showing good results, by not predicting failures on the simulations of CABRI REP-Na3, REP-Na4 and REP-Na5 (non-failed experiments), and predicting failure with 5.78% of deviation in deposited energy from the value reported for the CABRI REP-Na10 experiment.

ACKNOWLEDGMENTS

This work was funded by the U.S. Department of Energy, as part of the Nuclear Energy University Program (DOE-NEUP) under grant # DE-NE0009130. This research made use of the resources of the High-Performance Computing Cen-

TABLE II. CABRI REP tests specific modeling parameters. (DE = Deposited Energy, PPN = Power Peak Node)

Parameter	REP-Na3	REP-Na4	REP-Na5	REP-Na10
Failure	No	No	No	Yes
Active length (mm)	440.8	563	563	559
Number of Fuel Pellets	32	41	41	39
Fuel Pellet height (mm)	13.59	13.74	13.74	14.25
Cladding thickness (mm)	0.596	0.578	0.578	0.575
Refabrication gas pressure (MPa)	0.31	0.302	0.302	0.301
Burnup (GWd/tU)	54	62	64	63
Oxide thickness (μm)	48	80	20	80
RIA pulse width (ms)	9.5	76.4	8.8	31
Pulse total DE (cal/g)	122.2	95	104	108
Pulse failure DE at PPN (cal/g)	-	-	-	65.8

ter at Idaho National Laboratory, which is supported by the Office of Nuclear Energy of the U.S. Department of Energy and the Nuclear Science User Facilities under Contract No. DE-AC07-05ID14517.

REFERENCES

1. C. LEMAIGNAN and A. T. MOTTA, "Zirconium alloys in nuclear applications," *Materials Science and Technology, A Comprehensive Treatment*, **10 B**, 1–51 (1994).
2. J. PAPIN, B. CAZALIS, J. FRIZONNET, J. DESQUINES, F. LEMOINE, V. GEORGENTHUM, F. LAMARE, and M. PETIT, "Summary and interpretation of the CABRI REP-Na program," *Nuclear Technology*, **157**, *3*, 230–250 (2007).
3. R. O. MEYER, R. K. MCCARDELL, H. M. CHUNG, D. J. DIAMOND, and H. SCOTT, "A regulatory assessment of test data for Reactivity Initiated Accidents," *Nuclear Safety*, **37**, 372–387 (1996).
4. R. O. MEYER, "An assessment of fuel damage in postulated reactivity-initiated accidents," *Nuclear technology*, **155**, *3*, 293–311 (2006).
5. P. CLIFFORD, "Pressurized-water reactor control rod ejection and boiling-water reactor control rod drop accidents," Tech. Rep. RG 1.236, United States Nuclear Regulatory Commission (2020).
6. L. O. JERNKVIST, A. R. MASSIH, and P. RUDLING, "A strain-based clad failure criterion for reactivity initiated accidents in light water reactors," Tech. Rep. No. SKI-R–04-32, Swedish Nuclear Power Inspectorate (2004).
7. K. R. B. NANTES, M. JIN, and A. T. MOTTA, "Modeling hydrogen localization in Zircaloy cladding subjected to temperature gradients," *Journal of Nuclear Materials*, **589**, *154853* (2024).
8. R. S. DAUM, D. W. BATES, D. A. KOSS, and A. T. MOTTA, "The influence of a hydrided layer on the fracture of Zircaloy-4 cladding tubes," *International Conference on Hydrogen Effects on Material Behavior and Corrosion Deformation Interactions, Sep 22-26, 2002, Moran, WY, United States*, pp. 249–258 (2003).
9. D. L. HAGRMAN and G. A. REYMANN, "MATPRO-Version 11: a handbook of materials properties for use in the analysis of light water reactor fuel rod behavior," Tech. Rep. NUREG/CR-0497, EG & G Idaho (2 1979).
10. T. LINK, D. KOSS, and A. MOTTA, "Failure of Zr Cladding under Transverse Plane-Strain Deformation," *Nuclear Engineering and Design*, **186**, 379–394 (1998).
11. R. L. WILLIAMSON, J. HALES, S. NOVASCONE, M. TONKS, D. GASTON, C. PERMANN, D. ANDRS, and R. MARTINEAU, "Multidimensional multiphysics simulation of nuclear fuel behavior," *Journal of Nuclear Materials*, **423**, *1-3*, 149–163 (2012).
12. V. BOBKOV, L. FOKIN, E. PETROV, V. POPOV, V. RUMIANTSEV, and A. SAVVATIMSKY, "Thermophysical properties of materials for nuclear engineering: a tutorial and collection of data," *IAEA-THPH* (2008).
13. W. G. LUSCHER and K. J. GEELHOOD, "Material property correlations: comparisons between FRAPCON-3.4, FRAPTRAN 1.4, and MATPRO," Tech. Rep. NUREG/CR-7024, Pacific Northwest National Lab.(PNNL), Richland, WA (United States) (2010).
14. A. L. GLENDENING, "Influence of Hydride" blisters" on the Failure of Zircaloy-4 Under Equal Biaxial Tension," (2004).